Development of the Chinese 50th Percentile Male Human Body Model

Tianya Du, Jiqng Chen, Fengchong Lan

I. INTRODUCTION

The research team, led by Professor Lan in South China University of Technology, has dedicated over one decade to working on the Chinese Human Body Model (CHUBM) project, developing the Chinese human body finite element model (FEM) and analysing the injury biomechanics in vehicle crashes under Chinese accident characteristics, which describe the common accident type, the vehicle type, the human characteristics and the road environment. The CHUBM has increased in complexity and biofidelity with each successive improvement (three model versions in total). This study sets out the development and the validations of the latest detailed Chinese 50th percentile male (M50) FEM for use in vehicle crash injury biomechanics research as a part of the CHUBM project. There are nearly 15 simulations in which the model has been tested; a small subset of them will be presented here.

II. METHODS

Developing the FEM

The full body model (FBM) was constructed from high-resolution CT data of a ChineseM50 human subject. A regional modelling approach was used wherein models of the head, neck, thorax, abdomen, pelvis and lower extremity were developed independently and integrated into a single FBM with the same global coordinate system. The point clouds with anatomical characteristics were extracted by the 3D image convention tool MIMICS™, and then smoothed and faired up in Geomagic Studio™. Surfaces were created by feeding the polygon data into the ANSYS™mesh generator. Geometrical features with unnatural disconnections in the generated surfaces (such as bends or projections) were repaired in reference to anatomical drawings and such like. Through block segmentation, dense volumetric meshes were created from the surfaces. Hypermesh™ was used for model refinements, material definition, loading and boundary conditions application. The modelling method was applied for each body and tissue part. This model contained about 565,364 elements and 542,628 nodes. Summary statistics of the FBM are shown in Fig. 1.

The head and neck models were initially developed in previous studies[1-2]. The latest version of the head model was modified by refining the mesh quality, adding structures like sphenoidal sinus and sutura, as shown in Fig. 2(a). Ligaments and fibers of the neck model were connected to the head model via nodal connections (Fig. 3(b)).In the torso model, the vertebrae were connected through disks, ligaments and facet joints by shared nodes. The interactions of the internal organs and vessels were also simulated with contact interfaces. The lumbar spine was integrated to the sacrum using a rigid body. In the Plex (Pelvis and Lower Extremity) region, main structures of the pelvis, including the sacrum, hip bone, tailbone, ala of ilium and pubic ramus, were built. Within the lower extremity, the knee ligaments, including the MCL, LCL, PCL, ACL, menisci and patellar tendon, were also developed. The main details of the FBM are listed in Table I below. Thus, a large number of distinct anatomical structures were modelled explicitly, rather than homogenising the body's anatomy.

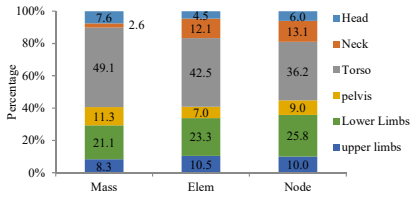

Fig. 1. Model mass, elements and nodes contribution by FBM.

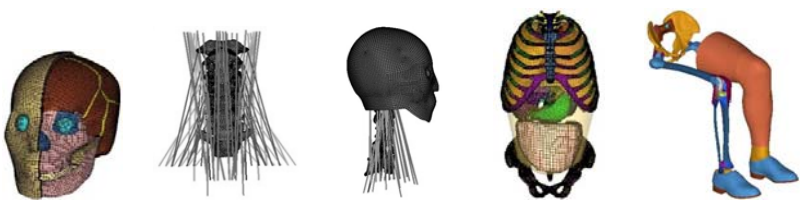

(a) (b) (c) (d)

Fig. 2. Body Region Models: (a) head model; (b) neck model; (c) torso model; (d) lower limbs model.

Fig. 3. Whole human body finite element model.

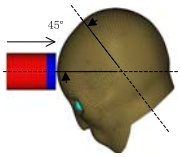

(a)

(b)

(c)

Fig. 4. Boundary conditions of validations: (a) head model; (b) torso model; (c) thigh model.

Material Modelling

The bony structures of the human model were assigned as elastic-plastic material characteristics, whereas incompressible material was assumed for the solid parts of organs. The soft tissues, such as muscles, internal contents, cerebrum, cerebellum and brainstem, were modelled as solid elements with linear viscoelastic material. The aorta, vena cava and the pleural membrane were modelled as shell elements with elastic material, as shown in Table I.

TABLE I
ELEMENT TYPE AND MATERIAL CHARACTERISTICS OF MAIN PARTS AND TISSUES

Tissues	Part	Element Type	Material Model	Density kg/mm^3	Young's Modulus(GPa)	Poison Ratio	Yield Stress (GPa)	Failure Strain
Spongy bone for vertebrae	Torso	Solid	Elastic-plastic	1.00E-06	1.00E+00	0.30	8.30E-03	-
Cortical bone for vertebrae	Torso	Solid	Elastic-plastic	2.75E-06	1.10E+01	0.20	2.50E-01	2.00E-02
Intervertebral disc	Torso	Solid	Elastic-plastic	1.20E-06	2.53E-01	0.40	1.40E-03	-
Spongy bone		Solid	Elastic-plastic	1.00E-06	4.00E-02	0.45	6.50E-03	2.00E-02
Cortical bone for ribs&sternum	Torso	Solid	Elastic-plastic	2.00E-06	1.15E+01	0.30	2.50E-01	3.00E-02
Spongy bone for pelvis	Pelvis	Solid	Elastic-plastic	1.00E-06	2.50E-02	0.30	1.00E-03	-
Cortical bone for pelvis	Pelvis	Solid	Elastic-plastic	2.00E-06	1.73E+01	0.30	1.00E-01	3.00E-02
Cortical bone for tibia	Lower limbs	Solid	Elastic-plastic	2.00E-06	1.31 E+01	0.30	1.21 E-01	1.5 E-02
Cortical bone for femur	Lower limbs	Solid	Elastic-plastic	2.00E-06	1.55 E+01	0.30	1.22 E-01	1.0 E-02
Cortical bone for fibula	Lower limbs	Solid	Elastic-plastic	2.00E-06	1.78 E+01	0.30	1.00 E-01	1.0 E-02
Cortical bone for patella	Lower limbs	Solid	Elastic-plastic	2.00E-06	1.55 E+01	0.30	1.10 E-01	-
Cerebrospinal fluid	Head	Solid	Elastic-fluid	1.04E-06	7.30E+00	0.45		
Blood	Torso	Solid	Elastic-fluid	1.00E-06	2.20E+00	0.45		
						G_0(MPa)	G_∞(MPa)	Damping Coefficient
Cerebrum	Head	Solid	Visco-elastic	1.14E-06	2.19E+00	1.00E-05	2.50E-05	8.00E-01
Cerebellum	Head	Solid	Visco-elastic	1.14E-06	2.19E+00	1.25E-05	2.50E-05	8.00E-01
Brainstem	Head	Solid	Visco-elastic	1.14E-06	2.19E+00	2.25E-05	4.50E-05	8.00E-01
Heart	Torso	Solid	Visco-elastic	1.00E-06	2.60E-03	4.40E-04	1.50E-04	2.50E-01
Lungs	Torso	Solid	Visco-elastic	6.00E-07	2.20E-04	2.00E-05	7.50E-05	2.50E-01
Liver, Spleen, Kidney	Torso	Solid	Visco-elastic	1.10E-06	2.80E-03	2.30E-04	4.40E-05	6.35E-01
Stomach	Torso	Solid	Visco-elastic	1.15E-06	1.45E-04	1.50E-05	5.00E-06	6.35E-01
Intercostal muscles	Torso	Solid	Visco-elastic	1.10E-06	2.10E-03	3.50E-04	8.20E-05	-
Rib cartilage	Torso	Solid	Elastic	1.60E-06	1.20E+00	0.20	-	-
Joint cartilage		Solid	Elastic	1.20E-06	9.70E-01	0.40	-	-
Ligament		Spring	Elastic	-	3.30E-02	-	-	-
Skin		Shell	Elastic	1.00E-06	3.15E-02	0.45	-	-
Cerebral dura mater	Head	Shell	Elastic	1.14E-06	3.15E-01	0.45	-	-

Cerebral pia mater	Head	Shell	Elastic	1.14E-06	1.15E-01	0.45	-	-
Cerebral falx	Head	Shell	Elastic	1.14E-06	3.15E-01	0.45	-	-
Diaphragm	Torso	Shell	Elastic	1.00E-06	6.55E-02	0.40	-	-
Aorta	Torso	Shell	Elastic	1.20E-06	5.00E-03	0.40	-	-
Vena cava	Torso	Shell	Elastic	1.00E-06	2.00E-02	0.40	-	-
Oesophagus	Torso	Shell	Elastic	1.00E-06	5.00E-03	0.40	-	-

Model validation against PMHS data

Post-mortem human subject (PMHS) tests on head, thorax and lower limbs were simulated to validate the responses of the models by comparing model predictions with experimental data. The head model validation was conducted with Nahum *et al.* experiment boundary conditions[3]. The simulation outcomes were compared with the experimental data in terms of the impact force history curve, the head gravity centre (HGC) acceleration history curve, and the pressure curves in forehead and occiput posterior fossa. The torso model was validated according to Kroell *et al.*'s experiments, and it was impacted at frontal speed of 6.7m/s[4]. Forces and force-deflections were obtained to decide the validity of the thorax model. The dynamic bending test was chosen to validate the thigh model in terms of force-displacement response[5].All the settings of simulations are shown in Fig. 4 above.

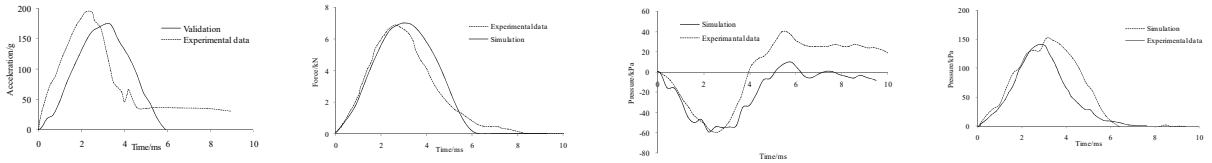

(a) (b) (c) (d)

Fig. 5. Head model validation results: (a) HGC acceleration comparisons; (b) contact force comparisons; (c) pressure in fossa comparisons; (d) pressure in forehead comparisons.

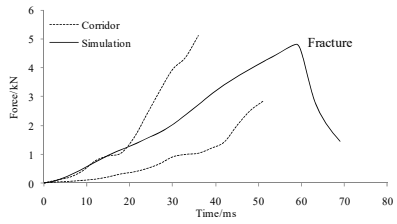

Fig. 6. Force comparisons in thigh model validation.

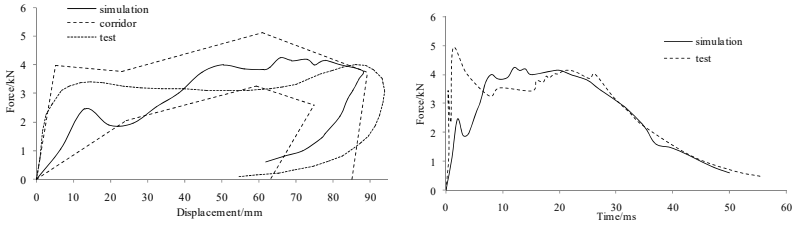

(a) (b)

Fig. 7.Torso model validation results: (a) force-deflection comparisons; (b)impact force comparisons.

III. DISCUSSION

The development and details of the M50 CHUBM were presented. In addition, three validation cases were investigated that separately highlight the kinematics and kinetics of the model. The model validation results showed relatively good agreement in these cases. It was useful to consider the mechanism of injuries incurred by analysing the results of the model validation simulations. While using cadaveric data for validating a human body model is the current standard in the field, there are limitations that coincide with using this data. Cadavers have both morphologic and material characteristics that make them unlike the living humans that any FBM ultimately aims to represent. Future studies will be more focused on biofidelity improvement and the analysis of material characteristics, but this lies outside the scope of the present study.

IV. REFERENCES

[1] Lei, S., South China University of Technology, 2011.
[2] Mengran, Z., South China University of Technology, 2011.
[3] Nahum, A.M.*et al.*,*Stapp Car Crash*, 1976.
[4] Kroell, C.K. *et al.*, *SAE Technical Paper*, 1974.
[5] Jason, R. K.*et al.*, *SAE Technical Paper*, 2003.